Free energy landscapes of model peptides and proteins

David A. Evans and David J. Wales
University Chemical Laboratories, Cambridge CB2 1EW, United Kingdom

(Received 13 November 2002; accepted 2 December 2002)

A parallel searching algorithm based on eigenvector-following is used to generate databases of minima and transition states for an all-atom model of the peptide $Ac(ala)_3NHMe$ and for a simplified bead model of a protein. We analyze the energy landscapes of both systems using disconnectivity graphs based upon both potential energy and free energy. This approach highlights the role of vibrational entropy in determining the relative free energy of local minima. Thermodynamic properties for $Ac(ala)_3NHMe$ calculated using the superposition approach are in reasonable agreement with parallel-tempering Monte Carlo simulations. © *2003 American Institute of Physics.* [DOI: 10.1063/1.1540099]

I. INTRODUCTION

Atomistic models are proving to be valuable tools in understanding the behavior of biological molecules. Characterizing the free energy landscape of model systems *via* simulation has enabled the thermodynamic properties and preferred conformations of peptide and small protein systems to be predicted.[1–3] Collecting trajectories of the system moving over the free energy landscape also allows predictions of kinetic properties to be made,[4] which of course is crucial to addressing the central question of how proteins can fold quickly and reliably to a single native structure.

Underlying every free energy surface is a potential energy surface (PES). Successful methods have been devised for mapping the PES of atomistic model systems and visualizing such multidimensional landscapes.[5,6] Furthermore, predictions of thermodynamic and kinetic properties can also be made based on the properties of the stationary points (minima and transition states) of the PES.[7]

In the current work we present a new representation of the free energy landscape of such systems, based upon the disconnectivity graph approach of Becker and Karplus,[5] and using harmonic densities of states to estimate the relative free energies of minima and transition states.[8] We apply this approach to two previously studied systems, and show how it highlights the importance of vibrational entropy in determining the relative free energy, and hence the occupation probability, of local minima.[9]

The first system we consider is a united-atom model of $Ac(ala)_3NHMe$. Ala_3 *in vacuo* with alternative capping groups was studied extensively in the development of a method for finding reaction paths on the PES.[10] The database obtained from this study was used in the first application of disconnectivity graphs.[5] This system is interesting because it represents the shortest peptide chain that can form an α-helical turn, although simulation studies have indicated that an extended conformation is actually preferred in aqueous solvent.[11] Larger polyalanine systems have also been studied to examine the apparent helix-stabilizing properties of the alanine residue, which is the simplest amino acid aside from glycine.[12,13] Mapping out the PES has provided predictions of thermodynamic and kinetic properties in continuum solvent models,[14–17] and simulations using Monte Carlo (MC) and molecular dynamics (MD) methods have also been undertaken.[13,18,19] In the present work results for thermodynamic properties calculated from databases of stationary points using the harmonic superposition approximation are compared with parallel-tempering MC simulations.[20] Parallel tempering, also known as replica-exchange,[21] has previously been combined with both MC and MD to obtain improved sampling of the configuration space of biomolecular systems.[22–24]

The second system we consider is a three-color 46-bead model, (*BLN*), which consists of 46 beads of three types: hydrophobic (*B*), hydrophilic (*L*), and neutral (*N*).[25] We employ a version of the potential in which the beads are linked by stiff springs.[26] The sequence is

$$B_9N_3(LB)_4N_3B_9N_3(LB)_5L. \tag{1}$$

This system has been studied by MD and MC methods, originally with the intention of analyzing a proteinlike model with several metastable free energy minima.[25,27] Subsequent studies have indicated the presence of two characteristic transition temperatures: collapse from an unfolded random coil to a compact globule, and folding of the globule to a β-barrel-like structure.[28–30] The PES of the system has also been studied,[26,31] and compared with the ''$\overline{\text{Go}}$'' version of the model where favorable non-native interactions are excluded and the system becomes less frustrated.[30,31] Two further studies considered self-assembly of the β strands[32] and the effect of mutation.[33] In the present work we demonstrate how the folding transition can be described in terms of sets of local minima on the PES.

II. ALANINE TETRAPEPTIDE

The $Ac(ala)_3NHMe$ system was modelled using a united-atom force field (CHARMM19)[34] and an implicit solvation potential.[35] The same system was previously studied by Krivov *et al.*[36] using Langevin dynamics and a confinement technique intended to give improved sampling of configuration space.

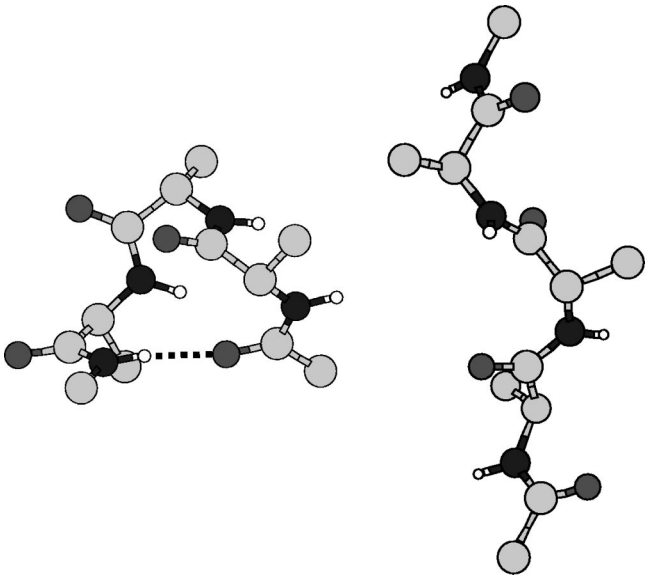

FIG. 1. The α (left) and β (right) strand minima of Ac(ala)$_3$NHMe. The α structure is the global potential energy minimum, and the β-strand structure is the global free energy minimum at 298 K. The dashed black line represents a hydrogen bond. This figure was prepared using Xmakemol (Ref. 53).

A. Landscape sampling

The global potential energy minimum for the system was located using the basin-hopping algorithm,[37] which is based on the Monte Carlo with minimization (MCM) method of Li and Scheraga.[38] Steps were taken by twisting one randomly chosen backbone dihedral angle by a random amount between $-180°$ and $+180°$. 100 runs of 10 000 steps each (at a temperature equivalent to 2.5 kcal mol^{-1} for the Metropolis acceptance criterion) all found the same lowest energy structure, which corresponds to one turn of an α-helix. This structure is shown in Fig. 1, and is apparently identical in geometry and energy to the global minimum reported previously.[36]

Starting from this global potential energy structure, a database of stationary points on the PES was constructed using the method described previously for polyalanine systems.[15,17] In brief, this approach involves building up a database of minima and transition states connected by steepest-descent paths, where minima and transition states are defined as stationary points on the potential energy surface with zero and one negative Hessian eigenvalues, respectively.[39] Analytic second derivatives of this potential are not available. Minima were located using the limited memory Broyden–Fletcher–Goldfarb–Shanno (L-BFGS) routine,[40] and transition states were located using the hybrid L-BFGS/L-BFGS technique, where one Hessian eigenvector is obtained by a variational method that does not require second derivatives.[41,42]

Up to forty transition state searches were initiated from each minimum in the database, which corresponds to twisting each of the 10 backbone dihedral angles (ϕ, ψ, and ω, the peptide bond) by $\pm 30°$ and $\pm 60°$. Propagation of the searches was carried out using a temperature of zero in the Metropolis criterion to decide whether to move to a newly found minimum, and the algorithm was run until 10 000 transition states had been located, resulting in a connected database of 1740 minima. All the stationary points were converged to a root-mean-square (RMS) gradient of less than 10^{-6} kcal mol^{-1} Å^{-1}, and vibrational frequencies were calculated by constructing and diagonalizing a Hessian matrix of mass-weighted two-sided numerical second derivatives. The whole procedure of database generation required about three days on sixteen UltraSparc II 400 MHz CPUs.

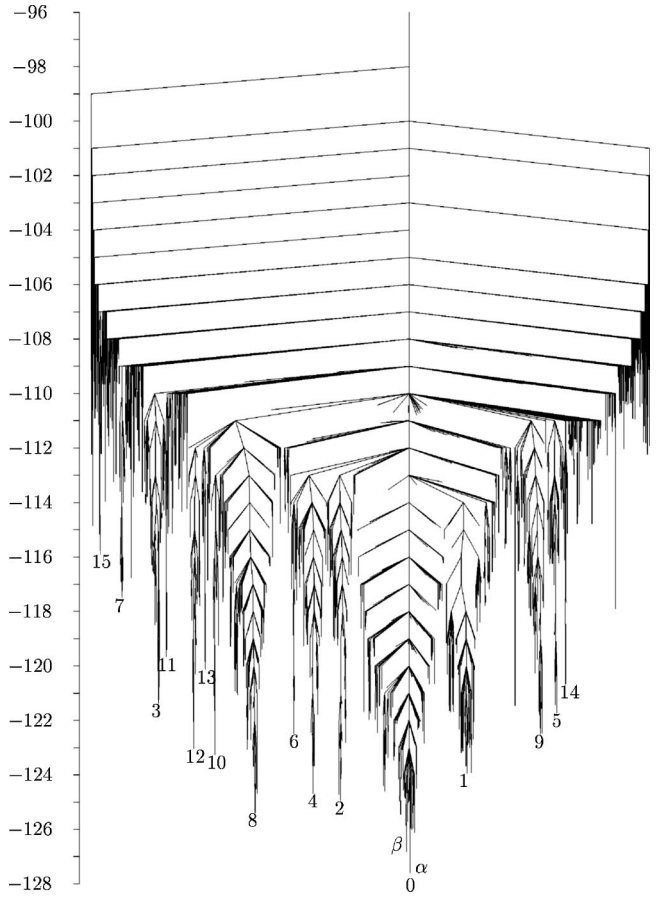

FIG. 2. Potential energy disconnectivity graph for Ac(ala)$_3$NHMe. The energy scale is in kcal mol^{-1}. α and β refer to the structures depicted in Fig. 1. The lowest 1200 minima are included. The numbers label the branches of the graph that contain the lowest minimum for each *cis-trans* isomer, as in Ref. 36.

B. Disconnectivity graphs

Connected databases, such as the one described above, are best visualized using disconnectivity graphs,[5] which partition the minima into disjoint sets based on the energies of the connecting transition states. The potential energy disconnectivity graph for the Ac(ala)$_3$NHMe database collected here is shown in Fig. 2. It is similar to the graph in Ref. 36, in that the lower part of the landscape is partioned into separate funnels for each peptide isomer.

Further insight can be gained into the thermodynamics and kinetics by considering a disconnectivity graph drawn on the basis of free energy. The relative free energies of minima and transition states can be estimated from their potential energy and normal mode frequencies according to the harmonic approximation to the density of states. The canonical

partition function, $Z_i(T)$, of minimum i at temperature T for a nonrotating system is given by

$$Z_i(T)=\frac{\exp(-E_i/k_BT)}{(h\overline{\nu_i}/k_BT)^{\kappa}}, \tag{2}$$

where E_i is the potential energy and $\overline{\nu_i}$ is the geometric mean normal mode frequency for minimum i. κ is the number of vibrational degrees of freedom ($3N-6$, where N is the number of atoms) and h is Planck's constant. We can also calculate the equilibrium occupation probabilities of each minimum,

$$P_i^{\mathrm{eq}}=\frac{Z_i(T)}{Z(T)}=\frac{Z_i(T)}{\Sigma_i Z_i(T)}, \tag{3}$$

where the sum is over every minimum i in the sample.

The canonical Rice–Ramsperger–Kassel–Marcus (RRKM) theory[43] rate constant out of minimum i through transition state † is

$$k_i^{\dagger}(T)=\frac{k_BT}{h}\frac{Z^{\dagger}(T)}{Z_i(T)}=\frac{(\overline{\nu_i})^{\kappa}}{(\overline{\nu^{\dagger}})^{\kappa-1}}e^{-(E^{\dagger}-E_i)/k_BT}. \tag{4}$$

The corresponding free energies of the minima and transition states can be defined as

$$F_i(T)=-k_BT\ln Z_i$$

and

$$F^{\dagger}(T)=-k_BT\ln Z^{\dagger}, \tag{5}$$

or

$$\begin{aligned} F_i(T)&=E_i+k_BT\ln(h\overline{\nu_i}/k_BT)^{\kappa},\\ F^{\dagger}(T)&=E^{\dagger}+k_BT\ln(h\overline{\nu^{\dagger}}/k_BT)^{\kappa-1}. \end{aligned} \tag{6}$$

From Eqs. (4) and (6) we obtain

$$k_BT\ln[hk_i^{\dagger}(T)/k_BT]=F_i(T)-F^{\dagger}(T), \tag{7}$$

which highlights the correspondence between the rate constant and the free energy difference. Due to the way we have defined $F^{\dagger}(T)$ it is possible for the free energy of a transition state to be less than the free energy of either or both of the minima that it connects. This result is not unphysical, it merely indicates a large rate at the chosen value of k_BT, and is unavoidable if we wish to plot $F^{\dagger}(T)$ on the same scale as $F_i(T)$. In order to construct disconnectivity graphs using the usual superbasin analysis,[5,7] we can add an arbitrary constant, f_c, to every transition state free energy, to ensure that each transition state lies above the minima it connects. The functions $F_i(T)$ and $F^{\dagger}(T)$ were used to construct the disconnectivity graph based on free energy shown in Fig. 3, for which $T=298$ K and $f_c=k_BT\ln[h5\times10^{12}\ \mathrm{s}^{-1}/k_BT]$. Only the 193 minima with an all-*trans* backbone (set 0 from Fig. 2) are included.

The method presented here differs from the canonical disconnectivity graphs described in Ref. 5, where the vertical scale represented k_BT. In the latter graphs all the minima were drawn at the same height at each temperature T, but grouped into nodes if they were interconnected by a path where $\max(\Phi_{ij}^{\dagger},\Phi_{ij}^{\dagger})<k_BT$, with $\Phi_{ij}^{\dagger}$ being the potential energy barrier going from minimum j to minimum i.

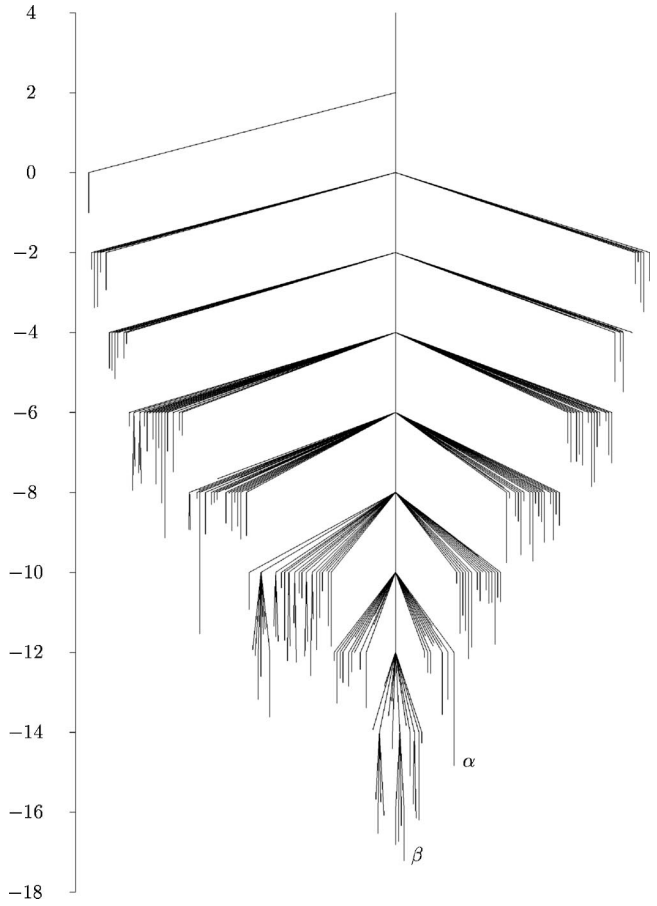

FIG. 3. Free energy disconnectivity graph for $Ac(ala)_3NHMe$ at 298 K. Only the all-*trans* minima are included. The energy scale is in kcal mol^{-1}. α and β refer to the structures depicted in Fig. 1.

It is desirable to coarse-grain samples of this size or larger so that only representative minima are displayed. An effective algorithm for coarse-graining samples of minima based on kinetic criteria has been presented previously.[44] This method groups any two minima i and j together if they are connected by a sequence of transition states for which all the forward and backward rate constants exceed a chosen threshold rate r_t. When plotting potential energy disconnectivity graphs, only the lowest energy minimum of each such group is then shown. In a further pruning step, if two groups are connected by a mechanism with rate greater than r_t in one direction, then the higher energy group is also excluded from the graph.

Having grouped the minima together in this way, it is straightforward to calculate the relative free energies of each group, and of the set of transition states that connect them. For group I we define

$$\begin{aligned} F_I^{\mathrm{group}}&=-k_BT\sum_{i\in I}\ln Z_i,\\ P_I&=\sum_{i\in I}P_i,\\ F_{IJ}^{\mathrm{group}}&=-k_BT\sum_{(i,j)^{\dagger}}\left[\frac{P_iP_j}{P_IP_J}\right]^{1/2}\ln Z^{\dagger}, \end{aligned} \tag{8}$$

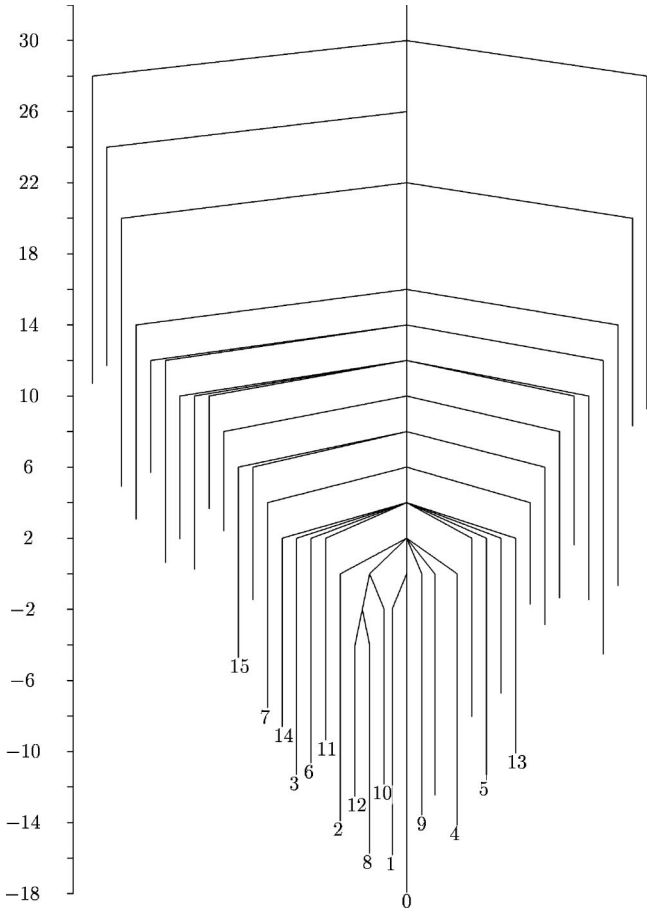

FIG. 4. Coarse-grained free energy disconnectivity graph for $Ac(ala)_3NHMe$ at 298 K. A rate threshold of 10^8 s^{-1} was used to group the minima as described in the text. The energy scale is in kcal mol^{-1}. Both α and β minima from Figs. 2 and 3 are included in the lowest group. The numbers label the branches of the graph that contain the lowest minimum of each *cis-trans* isomer, as for Fig. 2.

where the sum is over all transition states that connect a minimum in group I with a minimum in group J. The free energy of a group will thus include a contribution from the vibrational entropy of each minimum, and will also account for the configurational entropy associated with multiple local minima.[45] We define F_{IJ}^{group} in this way to reflect the contribution of each individual transition state to the intergroup rate constants, k_{JI} and k_{IJ}:

$$k_{JI}=\sum_{(i,j)^{\dagger}}\frac{P_i}{P_I}k_i^{\dagger}, \tag{9}$$

assuming all minima i in group I are in mutual equilibrium.[46,47]

Figure 4 represents the same database of minima as Fig. 3, but coarse grained with a rate threshold r_t of 10^8 s^{-1} and plotted using the resulting F_I^{group} and F_{IJ}^{group}. The lowest free energy group in fact contains 228 local minima, and lies 2.11 kcal mol^{-1} below the next lowest group. In equilibrium, at 298 K, 94.6% of the sample will be in the lowest group, according to the harmonic approximation for the density of states.

A similar grouping of local minima has been discussed in the context of kinetic MC simulations of diffusion processes.[46] Eigenvalues of the rate matrix **k**, with elements k_{ij}, where k_{ij} is the rate constant for a transition between minimum j and minimum i, and $k_{ii}=-\Sigma_{j\neq i}k_{ij}$, were used to choose appropriate rate constant thresholds. This approach was not used here because there were no clear breaks in the eigenvalue spectrum obtained by diagonalization of **k** for this system at $T=298$ K. Instead, r_t was chosen simply to illustrate how the graph may be simplified. In general, if a separation of time scales exists, a suitable grouping method should lend further meaning to free energy disconnectivity graphs.

C. Parallel-tempering simulations

Having calculated the partition functions of the minima using Eq. (2) it is straightforward to predict the equilibrium occupation probabilities of each minimum [Eq. (3)]. These can be computed at any temperature from the same data (potential energies and vibrational frequencies), though there will obviously be a limited range of temperature where the classical harmonic approximation is valid. To compare with these occupation probabilities we carried out parallel-tempering MC simulations, using the same potential as above and the CHARMM program.[48] The MC move set consisted of Cartesian displacements of all atoms, rotation of the backbone dihedral angles and concerted rotation of sections of the backbone, chosen with a probability based on the number of degrees of freedom involved and with attempt frequencies adjusted dynamically to give an acceptance ratio of 0.5. Eight replicas were run simultaneously for 1.1×10^7 MC steps, with temperatures ranging from 298 to 500 K. The temperatures were exponentially spaced, which should result in equal acceptance probabilities for each adjacent pair of temperatures.[23,49] After 10^6 equilibration steps exchange steps between replicas adjacent in temperature were attempted every 1000 regular MC steps (alternating between the [0–1, 2–3, ...] and [1–2, 3–4, ...] pairs). Energy minimization was also carried out every 1000th step from the instantaneous configuration in each run. Statistics were collected after a further 10^6 MC steps of equilibration. The number of times the system was found in the basin of attraction of each minimum, normalized by the total number of minimizations, defines the occupation probability of that minimum at any given temperature.

D. Discussion

Comparing the potential energy and free energy disconnectivity graphs (Figs. 2 and 3) shows that the global minimum (the node at the bottom of the graph) is different. The global free energy minimum at 298 K is an extended structure, which has a significantly lower mean vibrational frequency compared to the α-helical potential energy global minimum (Fig. 1). This result agrees with previous work,[36] where the extended structure is described as a β strand, although there is no hydrogen bonding of the sort associated with β sheets or hairpins in a typical protein structure. It appears that in this system increased conformational flexibility (higher vibrational entropy) outweighs the energetic benefit of forming hydrogen bonds.

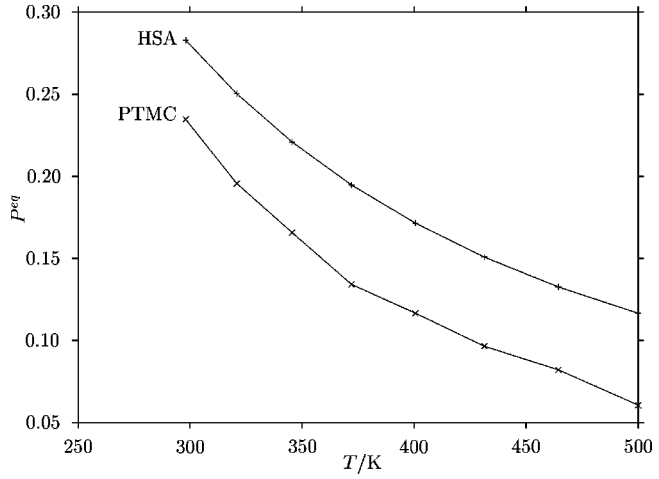

FIG. 5. Plot of the equilibrium occupation probability (P^{eq}) versus temperature as obtained by both the harmonic superposition approximation (HSA) and parallel-tempering Monte Carlo (PTMC).

The variation of the equilibrium occupation probability of the global free energy minimum (the β-strand structure) with temperature is plotted in Fig. 5. Results from both the harmonic superposition approach and the parallel tempering simulations are plotted and exhibit the same trend. Analysis of the simulation data shows that more than 99% of the minima found in each MC run were included in the database of 1740 minima found by the landscape searching algorithm. This high percentage suggests that the systematic discrepancy between the equilibrium occupation probabilities obtained with the two methods is due to inadequacies in the harmonic approximation to the density of states, rather than incomplete sampling of configuration space.

The structure of the most probable conformation can be compared with the results of a previous MD study for Ala_3 with terminal $-NH_3^+$ and $-COOH$ groups, which used explicit water molecules and a different force field.[11] This analysis showed that two conformers dominated at 300 K—the structure with central dihedral angles $(\phi,\psi)=(-120°,-170°)$, which these authors refer to as β, and the P_{II} structure with $(\phi,\psi)=(-70°,130°)$. In fact, the global free energy minimum of the present study corresponds to the P_{II} structure in the notation of Ref. 11, but we have found no evidence of significant population of any minima similar to the previous authors' β structure.

III. *BLN* MODEL

Previous work reported the construction and visualization of a connected database of minima for a continuum three-color 46-bead model protein.[31] The potential function used is given in Ref. 31, and we discuss here only the full, non-Go system. The model was originally proposed and studied with rigid bonds between the beads,[25,28–30] but here we use stiff harmonic bonds, as introduced by Berry *et al.*[26] The energy parameter ϵ determines the strength of the nonbonded interactions, which are modelled by a Lennard-Jones potential (see Ref. 31). We work here in reduced units of ϵ for the energy and σ for the distance and assume the particles have unit mass m.

The global potential energy minimum of this model is a four-stranded β barrel, and this was used as the starting point for the landscape searching algorithm. Re-examination of the database constructed in Ref. 31 revealed a wide range of mean vibrational frequencies for the various minima, which suggests that a better picture of the equilibrium conformational preferences of the system might be provided by a free energy disconnectivity graph of the type described in Sec. II B. Calculation of the relative free energies of all the minima in the database [*via* Eq. (6)] revealed that the global potential energy minimum is not the most occupied until the temperature drops below a value corresponding to 0.2ϵ. The physically interesting temperature regime appears to be from 0.1 to 1.0ϵ, based upon simulations of the same model.[25,28–30] In particular, two finite size phase transitions have been observed: collapse from random coil to compact globule at $T_\theta/\epsilon\approx 0.6$, and folding to a unique native structure at $T_f/\epsilon\approx 0.35$.[29] We show here that the T_f transition can be described using the connected database of minima.

Visualizing the free energy as a function of one or two order parameters has proved insightful in previous studies of biological molecules.[1–3] Here we have considered the equilibrium occupation probabilities, which are directly related to the local free energies, as a function of two order parameters, namely χ,[28] which is a measure of the structural similarity to the global potential energy minimum, and R_g, the radius of gyration. The probability distributions were constructed as

$$P(\chi)=\sum_i P_i\delta(\chi-\chi_i), \tag{10}$$

where χ_i is the order parameter (defined in Ref. 28) evaluated at minimum i, and similarly for R_g. Plots of $P(R_g)$ reveal a single large peak around 3σ, the value at the global minimum, for all temperatures that we considered, indicating that the unfolded region of the system has not been sampled. However, plots of $P(\chi)$ reveal a transition between two states corresponding to $\chi\approx 0$ and $\chi\approx 0.65$. In Fig. 6 a histogram of $P(\chi)$ is plotted for $T/\epsilon=0.24$, which is roughly the midpoint of the transition, determined as the temperature at which the areas under the two peaks in the histogram are equal.

A free energy disconnectivity graph for $T/\epsilon=0.24$ is shown in Fig. 7. This graph was coarse-grained using the approach described in Sec. II B and a rate-constant threshold of $10^{-6}(\epsilon/m\sigma^2)^{1/2}$, which groups the 500 local minima into 15 sets. We focus upon the two lowest-lying groups, with occupation probabilities 0.60 (group 1) and 0.25 (group 2) at the transition temperature, and calculate the expectation value of χ for each one using

$$\langle\chi\rangle=\frac{\Sigma_i\chi_i P_i}{\Sigma_i P_i}. \tag{11}$$

$\langle\chi\rangle=0.14$ and 0.65 for groups 1 and 2, respectively, and group 1 contains the global potential energy minimum, for which $\chi=0$ by definition. Together with the occupation probabilities these results strongly suggest that the folding

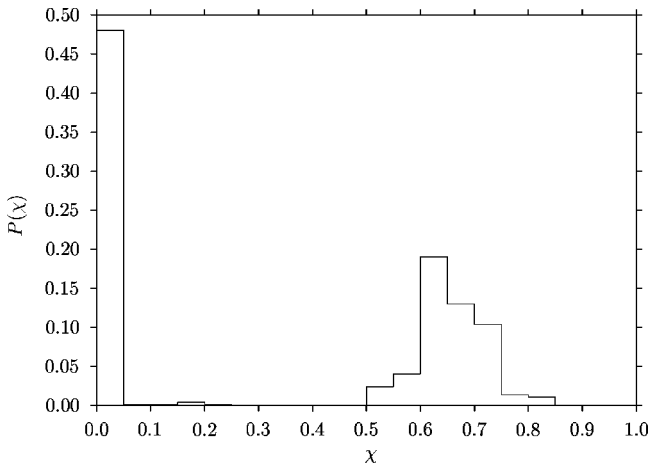

FIG. 6. Histogram of the probability distribution for the order parameter χ for the database of minima in the *BLN* system at $T/\epsilon=0.24$.

transition can be described in terms of the local minima in groups 1 and 2. The transition temperature calculated in the present work is probably lower than the value from simulation because of the harmonic approximation employed for the density of states.

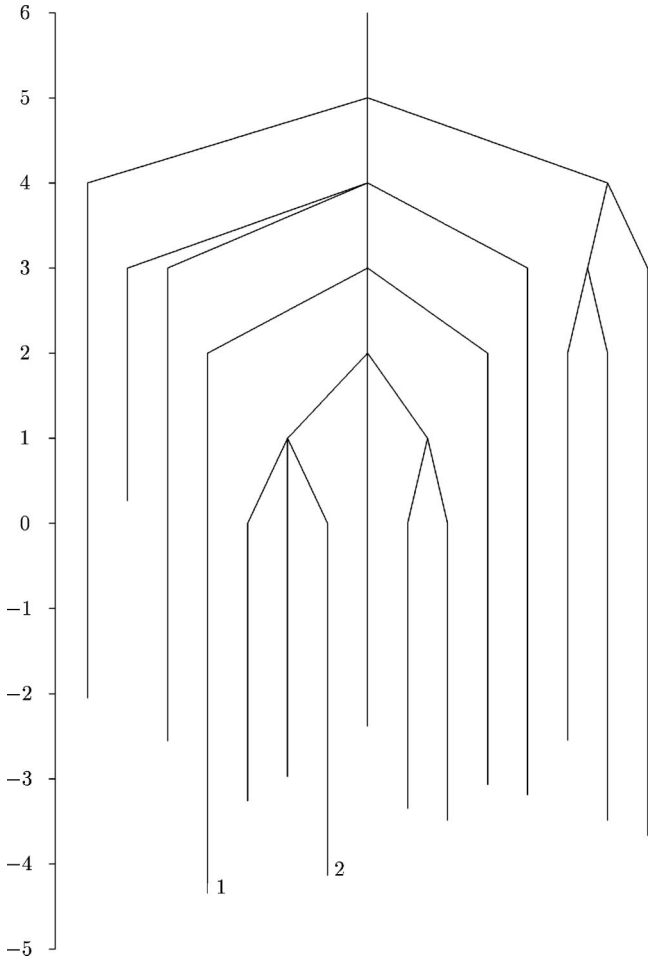

FIG. 7. Coarse-grained free energy disconnectivity graph for *BLN* at $T/\epsilon=0.24$. A rate threshold of 10^{-6} $(\epsilon/m\sigma^2)^{1/2}$ was used to group the minima as described in the text. The energy scale is in ϵ.

IV. CONCLUSIONS

Free energy disconnectivity graphs, a novel representation of the free energy landscape in terms of the partition functions of local minima and transition states, have been shown to provide new insight into two model systems. In $Ac(ala)_3NHMe$ we find that the significant regions of configuration space can be determined by considering the relative energy and mean vibrational frequencies of local minima on the PES. Extended structures, such as the β strand, have a higher vibrational entropy and hence can have higher equilibrium occupation probabilities than structures lower in potential energy, such as the α helix (see Fig. 1). This effect can be considered distinct from the higher configurational entropy associated with disordered regions of conformation space, such as an unfolded protein or a liquid phase, which arises from having more local minima associated with such regions.

Configurational entropy can be taken into account in free energy disconnectivity graphs if minima are grouped together appropriately; the free energy of a group of minima can be calculated from the partition functions of all the minima in the group. We have shown that a grouping method based upon the topology of the PES, described by the rate constants for interconversion of local minima, provides a description of the folding transition in the *BLN* system by isolating two groups of minima of roughly equal free energy at the transition temperature.

We expect that the free energy disconnectivity graph approach will prove useful for analyzing any system for which a connected database of minima and transition states can be constructed. The method should also help to explain the kinetics of such systems, as the barrier heights that determine the graphs are related to the rate constants for interconversion between groups of minima. In particular, one can predict that for any system described as two-state[50,51] it should be possible to find two corresponding groups of local minima with equal free energies.

Note added in proof: Since completing this work, a closely related method for constructing free energy disconnectivity graphs has been published by Krivov and Karplus.[52] These authors calculated free energy barriers by combining the contributions of different paths and compared the resulting disconnectivity graphs with those obtained using the lowest barrier, which is the method used in the present work.

ACKNOWLEDGMENTS

D.A.E. is grateful to the EPSRC for financial support. We thank Professor Martin Karplus and Dr. Sergei Krivov for helpful comments and comparison of results which helped us to correct an early version of the disconnectivity graph for the alanine tetrapeptide, Dr. Mark Miller for the use of his *BLN* database as well as numerous utility programs for database analysis, Dr. Paul Mortenson for the use of his parallel landscape searching program and Dr. Jon Doye and Dr. Florent Calvo for helpful discussions.

[1] E. M. Boczko and C. L. Brooks III, Science **269**, 393 (1995).
[2] B. D. Bursulaya and C. L. Brooks III, J. Am. Chem. Soc. **121**, 9947 (1999).
[3] A. R. Dinner, T. Lazaridis, and M. Karplus, Proc. Natl. Acad. Sci. U.S.A. **96**, 9068 (1999).
[4] B. Zagrovic, E. J. Sorin, and V. Pande, J. Mol. Biol. **313**, 151 (2001).
[5] O. M. Becker and M. Karplus, J. Chem. Phys. **106**, 1495 (1997).
[6] D. J. Wales, M. A. Miller, and T. R. Walsh, Nature (London) **394**, 758 (1998).
[7] D. J. Wales, J. P. K. Doye, M. A. Miller, P. N. Mortenson, and T. R. Walsh, Adv. Chem. Phys. **115**, 1 (2000).
[8] M. R. Hoare, Adv. Chem. Phys. **40**, 49 (1979).
[9] J. P. K. Doye and F. Calvo, J. Chem. Phys. **116**, 8307 (2002).
[10] R. Czerminski and R. Elber, J. Chem. Phys. **92**, 5580 (1990).
[11] Y. Mu and G. Stock, J. Phys. Chem. B **106**, 5294 (2002).
[12] J. S. Miller, R. J. Kennedy, and D. S. Kemp, Biochemistry **40**, 305 (2001).
[13] J. A. Vila, D. R. Ripoll, and H. A. Scheraga, Proc. Natl. Acad. Sci. U.S.A. **97**, 13075 (2000).
[14] Y. Levy, J. Jortner, and O. M. Becker, Proc. Natl. Acad. Sci. U.S.A. **98**, 2188 (2001).
[15] P. N. Mortenson and D. J. Wales, J. Chem. Phys. **114**, 6443 (2001).
[16] Y. Levy, J. Jortner, and O. M. Becker, J. Chem. Phys. **115**, 10533 (2001).
[17] P. N. Mortenson, D. A. Evans, and D. J. Wales, J. Chem. Phys. **117**, 1363 (2002).
[18] G. Hummer, A. E. García, and S. Garde, Phys. Rev. Lett. **85**, 85 (2000).
[19] G. Hummer, A. E. García, and S. Garde, Proteins: Struct., Funct., Genet. **42**, 77 (2001).
[20] E. Marinari and G. Parisi, Europhys. Lett. **19**, 451 (1992).
[21] K. Hukushima and K. Nemoto, J. Phys. Soc. Jpn. **65**, 1604 (1996).
[22] U. H. E. Hansmann, Chem. Phys. Lett. **281**, 140 (1997).
[23] Y. Sugita and Y. Okamoto, Chem. Phys. Lett. **314**, 141 (1999).
[24] R. Zhou, B. Berne, and R. Germain, Proc. Natl. Acad. Sci. U.S.A. **98**, 14931 (2001).
[25] J. D. Honeycutt and D. Thirumalai, Proc. Natl. Acad. Sci. U.S.A. **87**, 3526 (1990).
[26] R. S. Berry, N. Elmaci, J. P. Rose, and B. Vekhter, Proc. Natl. Acad. Sci. U.S.A. **94**, 9520 (1997).
[27] J. D. Honeycutt and D. Thirumalai, Biopolymers **32**, 695 (1992).
[28] Z. Guo and D. Thirumalai, Biopolymers **36**, 83 (1995).
[29] Z. Guo and C. L. Brooks III, Biopolymers **42**, 745 (1997).
[30] H. Nymeyer, A. E. García, and J. N. Onuchic, Proc. Natl. Acad. Sci. U.S.A. **95**, 5921 (1998).
[31] M. A. Miller and D. J. Wales, J. Chem. Phys. **111**, 6610 (1999).
[32] B. Vekhter and R. S. Berry, J. Chem. Phys. **110**, 2195 (1999).
[33] B. Vekhter and R. S. Berry, J. Chem. Phys. **111**, 3753 (1999).
[34] B. R. Brooks, R. E. Bruccoleri, B. D. Olafson, D. J. States, S. Swaminathan, and M. Karplus, J. Comput. Chem. **4**, 187 (1983).
[35] M. Schaefer, C. Bartels, and M. Karplus, J. Mol. Biol. **284**, 835 (1998).
[36] S. V. Krivov, S. F. Chekmarev, and M. Karplus, Phys. Rev. Lett. **88**, 038101 (2002).
[37] D. J. Wales and J. P. K. Doye, J. Phys. Chem. A **101**, 5111 (1997).
[38] Z. Li and H. A. Scheraga, Proc. Natl. Acad. Sci. U.S.A. **84**, 6611 (1987).
[39] J. N. Murrell and K. J. Laidler, Trans. Faraday Soc. **64**, 371 (1968).
[40] D. Liu and J. Nocedal, Math. Program. **45**, 503 (1989).
[41] L. J. Munro and D. J. Wales, Phys. Rev. B **59**, 3969 (1999).
[42] Y. Kumeda, L. J. Munro, and D. J. Wales, Chem. Phys. Lett. **341**, 185 (2001).
[43] R. G. Gilbert and S. C. Smith, *Theory of Unimolecular and Recombination Reactions* (Blackwell, Oxford, 1990).
[44] T. F. Middleton, J. Hernandez-Rojas, P. N. Mortenson, and D. J. Wales, Phys. Rev. B **64**, 184201 (2001).
[45] F. H. Stillinger and T. A. Weber, Phys. Rev. A **25**, 978 (1982).
[46] R. Q. Snurr, A. T. Bell, and D. N. Theodorou, J. Phys. Chem. **98**, 11948 (1994).
[47] M. L. Greenfield and D. N. Theodorou, Macromolecules **31**, 7068 (1998).
[48] A. R. Dinner, Ph.D. thesis, Harvard University, 1999.
[49] D. A. Kofke, J. Chem. Phys. **117**, 6911 (2002).
[50] S. E. Jackson and A. R. Fersht, Biochemistry **30**, 10428 (1991).
[51] A. R. Fersht, *Structure and Mechanism in Protein Science* (W. H. Freeman, New York, 1999).
[52] S. V. Krivov and M. Karplus, J. Chem Phys. **117**, 10894 (2002).
[53] M. P. Hodges, XMakemol: A program for visualizing atomic and molecular systems, version 4, Nottingham, 1999.